Journal Pre-proofs

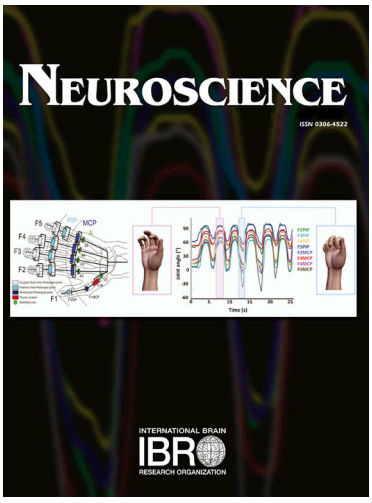

Research Article

Elevated acute plasma miR-124-3p level relates to evolution of larger cortical lesion area after traumatic brain injury

Niina Vuokila, Shalini Das Gupta, Riina Huusko, Jussi Tohka, Noora Puhakka, Asla Pitkänen

PII: S0306-4522(20)30138-X
DOI: https://doi.org/10.1016/j.neuroscience.2020.02.045
Reference: NSC 19553

To appear in: *Neuroscience*

Received Date: 20 August 2019
Accepted Date: 27 February 2020

Please cite this article as: N. Vuokila, S.D. Gupta, R. Huusko, J. Tohka, N. Puhakka, A. Pitkänen, Elevated acute plasma miR-124-3p level relates to evolution of larger cortical lesion area after traumatic brain injury, *Neuroscience* (2020), doi: https://doi.org/10.1016/j.neuroscience.2020.02.045

Elevated acute plasma miR-124-3p level relates to evolution of larger cortical lesion area after traumatic brain injury

Niina Vuokila[1¶], Shalini Das Gupta[1¶], Riina Huusko[2], Jussi Tohka[1], Noora Puhakka[1], Asla Pitkänen[1*]

[1]*A. I. Virtanen Institute for Molecular Sciences, University of Eastern Finland, PO Box 1627, FI-70211 Kuopio, Finland*

[2]*Natural Resources Institute Finland (Luke), PO Box 413, FI-90014 Oulu, Finland*

[¶]These authors contributed equally to this work

***Corresponding author:** Asla Pitkänen, MD, PhD, A. I. Virtanen Institute for Molecular Sciences, University of Eastern Finland, PO Box 1627, FI-70211 Kuopio, Finland, Tel: +358-50-517 2091, Fax: +358-17-16 3030, E-mail: asla.pitkanen@uef.fi

Short title: Acute circulating miR-124-3p levels associate with chronic cortical lesion area development.

Abstract

Mechanisms initiated by traumatic brain injury (TBI), leading to the development of progressive secondary injury are poorly understood. MicroRNAs (miRNAs) have a proposed role in orchestrating the post-injury aftermath as a single miRNA can control the expression of several genes. We hypothesized that the post-injury level of circulating brain-enriched miR-124-3p explains the extent of post-TBI cortical lesion. Three separate cohorts of adult male Sprague-Dawley rats (total n=57) were injured with lateral fluid-percussion–induced TBI. The miR-124-3p levels were measured in whole blood and/or plasma in cohorts 1 and 2 before TBI as well as at 2 d, 7 d, 2 months or 3 months post-TBI. The third cohort (22/57) was imaged with T2-weighted magnetic resonance imaging (MRI) at 2 months post-TBI to quantify cortical lesion area and perilesional T2-enhancement volume. Our data shows that miR-124-3p levels were elevated at 2 d post-TBI in both blood (FC 4.63, $p<0.01$) and plasma (FC 1.39, $p<0.05$) as compared to controls. Receiver operating curve (ROC) analysis indicated that plasma miR-124-3p level of 34 copies/µl or higher differentiated TBI animals from controls [area under curve (AUC) 0.815, $p<0.05$]. The data was validated in the third cohort (FC 1.68, $p<0.05$). T2-weighted MRI revealed inter-animal differences in cortical lesion area. Linear regression analysis revealed that higher the plasma miR-124-3p level at 2 d post-TBI, larger the lesion area at chronic time point ($R^2=0.327$, $p<0.01$). Our findings indicate that the extent of lateral fluid-percussion injury-induced chronic cortical pathology associated with the acutely elevated plasma miR-124-3p level.

Key words

microRNA; miR-124-3p; plasma; prognostic biomarker; receiver operating characteristic curve; traumatic brain injury

Abbreviations

A_{infl}, area of T2 enhancement; AIP, agranular insular cortex, posterior area; Au1, primary auditory cortex; AUC, area under curve; AuD, secondary auditory cortex, dorsal area; AuV, secondary auditory cortex, ventral area; BL, baseline; Ct, cycle threshold; CX_{contra}, volume of contralateral cortex; CX_{ipsi}, volume of ipsilateral cortex; d, days; ddPCR, droplet digital polymerase chain reaction; DI, dysgranular insular cortex; Ect, ectorhinal cortex; FPI, fluid percussion injury; GI, granular insular cortex; Hc, hippocampus; LPtA, lateral parietal association cortex; mo, months; MRI, magnetic resonance imaging; NISSL, Nissl staining; PRh, perirhinal cortex; PtPD, parietal cortex, posterior area, dorsal part; PtPR, parietal cortex, posterior area, rostral part; rf, rhinal fissure; RT-qPCR, reverse transcriptase quantitative polymerase chain reaction; S, sham-operated control; S1, primary somatosensory cortex; S1BF, primary somatosensory cortex, barrel field; S1ULp, primary somatosensory cortex, upper lip region; S2, secondary somatosensory cortex; sham, sham-operated control rat; T, TBI-induced animal; TBI, traumatic brain injury; TeA V1, primary visual cortex; Tha, thalamus; V, lateral ventricle; VIF, variance inflation factor, V1, primary visual cortex; V1B, primary visual cortex, binocular area; V1M, primary visual cortex, monocular area; V2L, secondary visual cortex, lateral area.

Introduction

Each year, 2.5 million individuals in Europe and the USA experience traumatic brain injury (TBI) (Taylor et al.,2017; Synnot et al., 2015). Over 40% of TBI patients report morbidities at the 1-y follow-up (Kersel et al., 2001). The severity and type of post-TBI neurologic and psychiatric morbidities relate to the location and severity of the primary and secondary injury in the brain (McAllister, 2011). Therapeutic approaches to improve recovery rely on alleviation of the secondary injury within a post-injury critical time window (Bayr et al., 2003, Bigler , 2001). Prediction of the severity of a secondary injury in a given subject, however, has been little investigated. Prognostic biomarkers that would pinpoint those individuals at highest risk of a large secondary brain injury would help to stratify subjects into those with the greatest need for tissue-preserving and recovery-enhancing therapies.

Secondary brain injury is the result of a symphony of activities of multiple molecular networks that lead to various cellular pathologies, including apoptosis, neuroinflammation, and mitochondrial dysfunction (Bramlett et al., 2015). MicroRNAs (miRNAs) are a class of small non-coding RNAs (~22 nt long) that regulate the expression of hundreds of messenger RNAs at the post-transcriptional level through messenger RNA degradation or translational repression (Bartel, 2004). Apart from cellular miRNAs, extracellular circulating miRNAs are observed in several body fluids such as serum, plasma, urine, and cerebrospinal fluid (Weber et al., 2010). Recently, miRNAs have emerged as diagnostic biomarkers for several diseases including cancer, cardiovascular disorders, and metabolic diseases, and potentially also brain diseases (Wang et al., 2016).

miR-124 is one of the most abundant and highly conserved miRNAs in the human and rodent brain (Lagos-Quintana et al., 2002; Sempere et al., 2004). Expression of miR-124 is considered crucial for normal neuronal differentiation and development (Visvanathan et al., 2007; Cheng et al., 2009; Åkerblom et al., 2012). Brain expression of miR-124 is also regulated in pathologic conditions with neuronal plasticity, including epileptogenesis after brain injury and glioma growth (Bot et al., 2013; Peng et al., 2013; Chen et al., 2015).

Several studies have reported the presence of miR-124 in the plasma after brain insults. For example, upregulated plasma levels of miR-124 are reported as early as 6 to 24 h after middle cerebral artery occlusion in rats (Laterza et al., 2009; Weng et al., 2011). Particularly, acute elevation in circulating miR-124 levels and its positive correlation with infarct volume has been observed in stroke studies (Sørensen et al., 2017). Recent studies demonstrated that elevated serum and plasma miR-124 levels correlate with the functional impairment

score and infarct volume and predict 3-month mortality after ischemic stroke in humans (Ji et al., 2016; Rainer et al., 2016).

The proposed presence of miR-124 in the exosomal fractions of human serum and plasma suggests its stability in the circulation (Huang et al., 2013; Ji et al., 2016). Further, no platelet or erythrocytic origin of miR-124 has been reported in plasma, which reduces the likelihood of false positive data related merely to sampling.

Based on these previous findings, we hypothesized that the post-TBI plasma miR-124-3p expression profile signals the magnitude of TBI-induced brain injury. We induced a lateral fluid-percussion injury (FPI) in adult rats, determined the cortical lesion volume and perilesional inflammation at 2 months post-TBI, and measured blood and plasma miR-124-3p levels at different post-TBI time-points. Our data shows that lateral FPI results in an acute elevation in blood and plasma miR-124-3p levels at 2 d post-TBI. Further, higher the plasma miR-124-3p level at the acute time, greater is the cortical lesion area developed at the chronic 2 months post-TBI time.

Materials and Methods

Animals

Animal numbers and study design are summarized in **Fig. 1.** Three separate cohorts of adult male Sprague-Dawley rats were used (cohort 1: n=30, body weight 337-384 g at the time of injury, Harlan Laboratories S.r.l., Horst, Netherlands; cohort 2: n=16, 381-425 g, Harlan Laboratories S.r.l., Udine, Italy; cohort 3: n=51, 347-425 g; Harlan Laboratories S.r.l., Udine, Italy). The initial body weight of the rats did not differ between cohorts ($p>0.05$). Rats were housed in a controlled environment (temperature 22 ± 1°C; humidity 50-60%; lights on from 07:00 to 19:00 h). Water and pellet food were provided *ad libitum*.

Follow-up of animal well-being. To minimize suffering and distress, overall well-being of the rat and its motor activity, eating and drinking, and the growth of teeth were observed daily. If an animal showed signs of pain (*e.g.,* weight loss, abnormal movement or posture, excessive grooming), it was treated with carprofen (Rimadyl®, 5 mg/kg, once per day for 3 days, Zoetis Finland Oy). Rats that were subjected to lateral fluid-percussion injury (FPI) received soft food and water from a serving dish placed on the floor of the cage until they were able to eat normal food (2-3 days). The weight was monitored 1 week before induction of TBI, on the day of surgery, daily for 7 d post-TBI, and thereafter, once per week for up to 9 weeks.

Pre-set humane end point. If the post-injury weight loss was more than 30%, the rat had to be euthanized using 4% isoflurane anesthesia followed by decapitation. None of the animals met this criterion.

TBI-related mortality. Based on previous experience with the model, we expected <10% anesthesia-related mortality, and 20-30% acute post-impact mortality (within 72 h) at impact level 3.3 atm (see Results).

All animal procedures, including acute mortality and humane end point, were approved by the Animal Ethics Committee of the Provincial Government of Southern Finland, and carried out in accordance with the guidelines of the European Community Council Directives 2010/63/EU.

Induction of TBI with lateral fluid-percussion

Rats were subjected to lateral fluid-percussion (FPI) -induced TBI (cohort 1: 17 rats, cohort 2: 10 rats, cohort 3: 30 rats) as described previously (McIntosh et al., 1989; Kharatishvili et al., 2006]). Briefly, the animals were anesthetized by intraperitoneal injection (6 ml/kg body weight) of a mixture containing sodium pentobarbital (58 mg/kg), magnesium

sulfate (127.2 mg/kg), propylene glycol (42.8%), and absolute ethanol (11.6%), and placed in a Kopf stereotactic frame (David Kopf Instruments, Tujunga, CA, USA). The anesthetic cocktail used in cohort 1 also contained 60 mg/kg chloral hydrate, but it was removed from the later experiments (cohorts 2 and 3), as its use was no longer permitted in our renewed animal license. A midline scalp incision was made, and the underlying periosteum removed. A circular craniectomy (diameter 5 mm) was performed with a trephine over the left hemisphere midway between lambda and bregma, with the lateral edge of the craniectomy adjacent to the lateral ridge. A modified Luer–lock cap was placed and sealed into the craniectomy site, cemented onto the skull (Selectaplus CN, Dentsply DeTRey GmbH, Dreieich, Germany) and filled with saline. At 90 min after injection of the anesthetics, the animals were connected to the fluid-percussion device (AmScien Instruments, Richmond, VA, USA) through the male Luer–lock fitting, and brain injury was induced (cohort 1 and cohort 3: 3.3 ± 0.01 atm, cohort 2: 3.2 ± 0.02 atm). Time in apnea and occurrence of acute post-impact seizure-like behavior was monitored. Sham-operated experimental controls (cohort 1: 13 rats, cohort 2: 6 rats, cohort 3: 14 rats) received anesthesia and all surgical procedures without lateral FPI. Cohort 3 also included 7 naïve animals that did not undergo any surgical procedures.

Sampling of whole blood, plasma, and brain tissue

Whole blood sampling with cardiac puncture. Cohort 1 served as a discovery cohort to analyze if the brain-enriched miR-124-3p level is detectable in circulation post-TBI. Analysis in this cohort was performed with whole blood. Whole blood was sampled at 2 d (7 TBI, 6 sham) and 2 months (9 TBI, 6 sham) post-TBI. After anesthetizing the rats with the anesthesia cocktail described above, an 18G needle (Terumo Neolus, Terumo Europe N.V., Leuven, Belgium) was placed into the left cardiac ventricle, and 3 ml of blood was drawn into a syringe and transferred to K_3 EDTA-tubes (tri-potassium ethylenediaminetetraacetic acid, BD Biosciences, Franklin Lakes, NJ). Blood samples were snap-frozen in liquid nitrogen and stored at -70°C until processed.

Plasma sampling from the tail vein. Tail vein plasma was sampled at 7 d before TBI (baseline), 2 d, 7 d and 3 months post-TBI according to principles of 3Rs (www.nc3rs.org.uk/rat-tail-vein-non-surgical) (cohort 2: 10 TBI, 6 sham; cohort 3: 22 TBI, 14 sham, 7 naïve). Cohort 2 served as the first validation cohort to confirm the elevated blood post-TBI miR-124-3p levels in plasma samples. Briefly, rats were anesthetized in 4.5% isoflurane in an induction chamber. The anesthesia was maintained through a nose mask

during the procedure. After positive findings in cohort 2, we extended the analysis to plasma samples collected from cohort 3.

In cohorts 2 and 3, blood (~500 µl) was drawn from the lateral tail vein into Microtainer K_2 EDTA-tubes (di-potassium ethylenediaminetetraacetic acid, Microtainer, BD Biosciences, Franklin Lakes, NJ) using a 25G butterfly needle (Surflo Winged infusion set, Terumo Europe N.V., Leuven, Belgium). Samples were centrifuged at 1300g (Centrifuge 5417R, Eppendorf Biotools, CA) at +4°C for 10 min, pipetted into Protein LoBind tubes (Eppendorf LoBind, Eppendorf AG, Hamburg, Germany) in 50-µl aliquots, frozen in dry ice, and stored at -70°C until processed.

Sampling of brain tissue. Rats were anesthetized with 4% isoflurane and their brains were quickly removed. Brains from cohort 3 were immersion-fixed in buffered 10% formalin and cryoprotected in 20% glycerol in potassium phosphate buffered saline (pH 7.4). Samples were stored at -70°C until processed. At the time of processing, brains were sectioned (1-in-6 series of coronal sections, 30 µm) with a sliding microtome (Leica SM 2000, Leica Microsystems Nussloch GmbH, Nussloch, Germany). The first series was stored in 10% buffered formalin at room temperature until Nissl staining. The remaining sections were stored in cryoprotectant solution (30% ethylene glycol, 25% glycerol on 0.05 M sodium phosphate buffer, pH 7.4) until further processed.

Extraction of total RNA from whole blood and plasma

Whole blood. Total RNA was extracted from 200 µl of 2 d or 2 months post-TBI blood using a miRNeasy Serum/Plasma Kit (Qiagen, Hilden, Germany; miRNeasy Serum/Plasma Handbook 02/2012; http://www.qiagen.com/us/). Briefly, blood cells were lysed with QIAzol Lysis Reagent. Total RNA (including small RNAs approximately ≥ 18nt) was extracted with chloroform and washed with ethanol. The RNA was bound to a RNeasy MinElute column and eluted with RNase-free water. After extraction, the eluent containing the RNA was diluted to 1:300.

Plasma. Total RNA was extracted from 50 µl of tail-vein plasma using the Exiqon miRCURY™ RNA isolation kit – biofluids (#300112*,* Exiqon*, Vedbæk, Denmark).* In cohort 2, RNA extraction was performed for all four time points (baseline, 2 d, 7 d and 3 months post-TBI). In cohort 3, RNA extraction was only performed for baseline and 2 d post-TBI samples. According to the protocol, the starting material was centrifuged at 3000g for 5 min to pellet any debris or insoluble cellular components. Each sample was then topped up with nuclease-free water to a final volume of 200 µl and mixed with 60 µl of the lysis solution

buffer. To enhance the isolation of low abundance miRNAs, 1 µg of MS2 carrier RNA (#10165948001, Roche Diagnostics GmbH, Mannheim, Germany) was added to each sample of cohorts 2 and 3. In cohort 2, 1 µl of the Exiqon RNA spike-in template mixture (#203203, Exiqon, Vedbæk, Denmark) was also added to each sample. The spike-in template was designed as a mix of three spike-ins, UniSp2, UniSp4, and UniSp5, such that UniSp2 was present at a concentration 100-fold higher than that of UniSp4, and UniSp4 was present at a concentration 100-fold higher than that of UniSp5. UniSp4 was subsequently chosen for polymerase chain reaction (PCR) amplification to monitor the efficiency of the RNA isolation step. In both cohorts, RNA was then extracted according to the manufacturer's instructions, with final elution in 25 µl of nuclease-free water to obtain a concentrated eluate of small RNAs, while larger RNAs were retained in the column. For long-term storage, purified RNA samples were kept at -70°C. All centrifugations were performed at room temperature. The optional proteinase K treatment was omitted in both cohorts. In cohort 3, synthetic spike-ins were not added.

Reverse transcription of RNA to cDNA

Reverse transcription (RT) of total RNA in whole blood samples using TaqMan chemistry

Total RNA was translated to complimentary DNA (cDNA) with a TaqMan miRNA Reverse Transcriptase Kit (#4366596, Applied Biosystems, Foster City, CA, http://www.appliedbiosystems.com), according to the manufacturer's instructions. The sample (15 µl) was prepared by mixing 7 µl of RT master mix with 5 µl of RNA solution (10 ng RNA in 5 µl nuclease-free water) and 3 µl of 5x-RT primer for miR-124-3p (mmu-miR-124-3p, #001182, Applied Biosystems). Then, RT was performed using a T100™ Thermal Cycler (Bio-Rad Laboratories Inc, Hercules, CA, USA) as follows: 16°C for 30 min, 42°C for 30 min, 85°C for 5 min and 4°C thereafter. Samples were stored at -20°C until further processed. U6 snRNA (snRNA U6, #001973, Applied Biosystems) was used as an endogenous control.

RT of total RNA in plasma using TaqMan and Exiqon chemistries

For RT of the synthetic spike-in UniSp4 that was added during RNA isolation to samples from cohort 2, we used the Exiqon miRCURY LNA™ Universal RT microRNA PCR protocol (Universal cDNA synthesis kit II, 8-64 reactions, #203301, Exiqon). The cDNA synthesis master mix was prepared according to the protocol guidelines using 5x reaction buffer, RT

enzyme mix, and nuclease-free water. A 1-µl aliquot of the UniSp6 synthetic RNA spike-in was added to each reaction to monitor the efficiency of the RT step. RT was performed with the following thermal cycling conditions: incubation for 60 min at 42°C, heat-inactivation of the reverse transcriptase for 5 min at 95°C, followed by immediate cooling to 4°C, and storage at -20°C.

RT for plasma miR-124-3p in cohorts 2 and 3 was performed using the TaqMan chemistry as for cohort 1, except that we used undiluted RNA eluate. Because hemolysis and release of miRNAs from blood cells can severely impair the detection of circulating miRNA biomarkers, RT of miR-23a (#000399, Applied Biosystems) and miR-451 (#001141, Applied Biosystems) was performed for samples in cohort 3 to calculate the hemolysis coefficient. Thermal cycling conditions were the same as for cohort 1 (T100™ Thermal Cycler, Bio-Rad Laboratories Inc). The cDNA samples thus obtained were stored at -20°C until further processed.

Analysis of copy number for circulating miR-124-3p with RT-qPCR and droplet digital PCR

RT-qPCR of miR-124-3p in whole blood

The miR-124-3p levels in whole blood sampled at 2 d or 2 months post-TBI was determined with RT-qPCR using the TaqMan Small RNA Assays protocol (Applied Biosystems, http://www.appliedbiosystems.com). Briefly, TaqMan Small RNA Assay (20x, mmu-miR-124-3p, #001182, UAAGGCACGCGGUGAAUGCC, Applied Biosystems, or snRNA U6, #001973, GTGCTCGCTTCGGCAGCACATATACTAAAATTGGAACGATACAGAGAAGATTAGCATG GCCCCTGCGCAAGGATGACACGCAAATTCGTGAAGCGTTCCATATTTT, Applied Biosystems) was mixed with 1.33 µl of RT product, TaqMan Universal PCR Master Mix II with no UNG, and nuclease-free water (Ambion,_AM9938, Thermo Fisher Scientific, Waltham, MA, USA) according to manufacturer's instructions. RT-qPCR was run using StepOnePlus™ Real-Time PCR System (Software v2.1, Applied Biosystems) with a standard program: 50°C for 2 min, 95°C for 10 min followed by 40 cycles (15 s each) at 95°C, and finally, at 60°C for 60 s. C_t values were normalized relative to snRNA U6 with the formula $2^{-\Delta Ct}$ (Carvalho-Caspar et al., 2005; Hata et al., 2008; Maru et al. 2009; Song et al., 2012). U6 is detected in blood cells (Yan et al., 2016) and small circulating vesicles (Savelyeva et al., 2017) and was thus used to normalize the miR-124-3p level in the whole blood. Because U6 has been deemed unsuitable for normalizing miRNA RT-qPCR data

from circulating biofluids like serum and plasma (Xiang M et al., 2014; Tang et al., 2015), it was not analyzed in cohorts 2 and 3.

RT-qPCR of miR-124-3p in plasma

TaqMan chemistry was applied for RT-qPCR amplification of miR-124-3p in plasma samples as described for whole blood (cohort 2: baseline, 2 d, 7 d and 3 months post-TBI; cohort 3: baseline and 2 d post-TBI). For amplification of the synthetic spike-ins UniSp4 (from the RNA isolation step) and UniSp6 (from the RT step), the miRCURY LNA™ Universal RT microRNA PCR system was used (ExiLENT SYBR® Green master mix, #203403, Exiqon). For this, the cDNA samples from Exiqon protocol were diluted to 40x in nuclease-free water. Because the Exiqon PCR Master Mix does not contain the passive reference dye, 0.2 µl of ROX (Invitrogen, Life Technologies, Carlsbad, CA, USA) per PCR replicate was also added to each of the diluted cDNA samples prior to PCR amplification. All amplifications were performed in triplicate. The 10-µl PCR reaction mixture was designed according to the protocol guidelines, and RT-qPCR amplification followed by melting curve analysis was then performed in the StepOnePlus™ Real-Time PCR system (Applied Biosystems). The thermal cycling conditions for RT-qPCR were as follows: polymerase activation/denaturation at 95°C for 10 min, followed by 40 amplification cycles at 95°C for 10 s, 60°C for 1 min (ramp rate 1.6°C/s).

Droplet digital PCR of miR-124-3p in plasma

For cohort 2, absolute quantification of the plasma miR-124-3p copy number was also performed with droplet digital PCR (ddPCR), for 2 d post-TBI samples. For this, 1.33 µl of undiluted cDNA template from the TaqMan RT reaction (same samples as above) was added to a 20-µl reaction mixture containing 10 µl Bio-Rad 2x ddPCR supermix for probes (#186-3010, Bio-Rad, CA USA), 1 µl 20x miR-124-3p PCR primer, and 7.67 µl nuclease-free water. The 20-µl reaction mixtures were loaded in disposable droplet generator cartridges (#186-4008, DG8™ Cartridges for QX100™/QX200™ Droplet Generator, Bio-Rad, Germany) along with 70 µl of droplet generation oil for probes (#186-3005, Droplet generation oil for probes, Bio-Rad, CA, USA). The cartridges were then covered with gaskets (#186-3009, Droplet Generator DG8™ Gaskets, Bio-Rad, CA, USA) and placed in the droplet generator (#186-3001, Bio-Rad QX100™ Droplet Generator, Solna, Sweden) to create oil-emulsion droplets. Once the droplets were generated, they were transferred to 96-well PCR plates (Twin. tec PCR plate 96, semi-skirted, colorless, Hamburg, Germany)

sealed, thermal cycled (96-well PTC-200 thermal cycler, MJ Research), and quantified at the end-point in the droplet reader (#186-3001, Bio-Rad QX100^{TM} Droplet Reader, Solna, Sweden) using QuantaSoft software (v1.7, Product code: 186-4011, Bio-Rad, CA, USA). The thermal cycling conditions for ddPCR were as follows: polymerase activation/denaturation at 95°C for 10 min, followed by 40 amplification cycles at 95°C for 15 s and 60°C for 1 min, with a final inactivation step at 98°C for 10 min. Because clusters of positive droplets appeared only above the amplitude threshold of 6000, the level was set to this value for all ddPCR runs to minimize false positives. For each sample, the reaction was performed in duplicate, and the sum of miR-124-3p copies/20-µl PCR reaction from the two replicates was calculated. From this, miR-124-3p copies/µl of original plasma used for RNA extraction was estimated and this parameter (miR-124-3p copies/µl plasma) was used for data representation in the figures.

Normalization of plasma miR-124-3p RT-qPCR data

As no generally accepted endogenous control is available, we normalized cohort 2 plasma miR-124-3p RT-qPCR levels to the synthetic spike-in UniSp4.

For normalization of miR-124-3p levels in cohort 3 samples (n=43), we made an effort to identify a suitable endogenous normalization control using the R-based NormFinder approach ((Tang et al., 2015), user guide: http://moma.dk/files/newDocOldStab_v5.pdf). NormFinder identified the stability value for miR-23a to be 0.31 (input to NormFinder= mean Ct of miR-23a in three technical replicates for each biologic sample), which was less than the arbitrary cut-off value, usually set at 0.4 (Tian et al., 2015). Consequently, miR-23a was selected as an endogenous control, and normalization of plasma miR-124-3p levels in cohort 3 was performed using the formula $2^{-\Delta Ct}$ (Carvalho-Caspar et al., 2005; Hata et al., 2008; Maru et al. 2009; Song et al., 2012). Since baseline levels of plasma miR-124-3p were not different between the sham and the TBI groups in both cohorts 2 and 3; we further normalized the plasma miR-124-3p levels in each animal by dividing the 2 d miR-124-3p levels by the baseline level ($2^{-\Delta Ct\ (2D)}$/ $2^{-\Delta Ct\ (BL)}$). This resulted in a relative value that was independent of the UniSp4 or miR-23a based normalization methodology. Plasma miR-124-3p levels were comparable in naïve and sham-operated animals in cohort 3 ($p>0.05$), and consequently, data from these groups was combined and referred to as controls in further analyses.

Quantification of hemolysis

TaqMan chemistry was used for RT-qPCR amplification of plasma hemolysis markers, miR-23a and miR-451 (see above) (Blondal et al., 2013; Shah et al., 2016). The hemolysis coefficient (cohort 3) was calculated as ΔC_t (miR-23a - miR-451) (Blondal et al., 2013; Shah et al., 2016). A sample was included in the study if ΔC_t <5.

Magnetic resonance imaging

T2-weighted MRI

To assess the lesion location and extent (including the width) of the perilesional inflammatory rim, T2-weighted magnetic resonance imaging (MRI) was performed at 2 months post-TBI in cohort 3 (22 TBI animals), using a 7 T Bruker Pharmascan MRI scanner equipped with a volume transmitter coil and surface receiver coil combo. Animals were anesthetized with isoflurane (4% for induction and 2% for maintenance during imaging) and positioned in a stereotactic holder. T2-weighted images were acquired with fast spin-echo from 25 slices (field of view (FOV) =30 mm x 30 mm, matrix slice thickness=1 mm, TR=4000 ms, TE=40 ms).

Analysis of MRI images

Location and area of cortical lesion. To assess the location and extent of the lesion area, we prepared 2-dimensional cortical unfolded maps using 1-mm-thick coronal MRI slices as described previously (Ndode-Ekane et al., 2017). The coordinates were determined based on the rat brain atlas by Paxinos and Watson (Paxinos et al., 2007). The unfolded maps were generated using the web-based software UnfoldedMap (http://unfoldedmap.org/, Andrade et al., 2018).

Volume of the remaining cortex and perilesional T2 enhancement. The analysis of MRI slices revealed substantial variability in the extent of the cortical lesion between the animals at 2 months post-TBI (**Fig. 2A**). Moreover, the distribution of the enhanced T2-weighted signal appeared unevenly distributed along the rostrocaudal extent of the cortical lesion. To assess the lesion heterogeneity in more detail, we measured the area of T2-weighted signal enhancement in the ipsilateral (perilesional) cortex, indicating an inflammatory response (A_{infl}) (**Fig. 2B**), at anteroposterior (AP) levels -2 to -7 mm from the bregma (according to rat brain atlas of Paxinos and Watson (Paxinos et al., 2007). The area of the ROIs was calculated from each section using an open source graphical tool for Matlab

(available: aedes.uef.fi). The volume of each ROI was calculated by a Cavalieri estimation as follows:

$$V(Cx) = \Sigma S(Cx) * t * a(s)$$

where ΣS(Cx)= the total number of cortical sections analyzed, t=section thickness (1 mm), and a(s)= the area of ROI (mm^2)(Gundersen et al., 1988a; Gundersen et al., 1988b; Schmitz et al., 2005).

Histologic analysis of tissue

To further characterize the lesion pathology, with focus on perilesional inflammation as suggested by signal enhancement in T2w MRI, we performed Nissl staining (see Huusko et al., 2013).

Statistical analysis

Statistical analyses were performed using IBM SPSS Statistics 25.0 (IBM Corp., Armonk, NY, USA). Data was visualized with GraphPad Prism version 8.0.2 (GraphPad Software, San Diego, California USA). Datasets were analyzed using the non-parametric Kruskal-Wallis ANOVA test followed by *post hoc* analysis with the Mann-Whitney *U* test. To explore relationships between the measured parameters, a multiple linear regression analysis was performed followed by a simple linear regression. A receiver operating characteristic (ROC) test was performed to investigate the sensitivity and specificity of miR-124-3p level as a prognostic biomarker for TBI lesion severity. A P-value less than 0.05 was considered statistically significant.

Results

Impact severity, mortality, duration of post-impact apnea, and occurrence of acute post-impact seizures

The animal numbers, sampling times, and follow-up mortality are summarized in **Fig. 1**.

Cohort 1. Impact severity was 3.3 ± 0.02 atm. Acute post-TBI mortality (<72 h) was 6% (1/17). In the sham-operated group, one rat died from an unknown cause during the surgery. The mean post-impact apnea time was 21 ± 2.6 s. Post-impact seizure-like behaviors were observed in 29% (5/17) of TBI animals.

Cohort 2. Impact severity was 3.2 ± 0.02 atm. Acute post-TBI mortality was 0% ($p>0.05$ as compared with cohort 1). The mean post-impact apnea time was 23 ± 2.1 s ($p>0.05$ as compared to cohort 1). Post-impact seizure-like behaviors were observed in 13% (2/16) of TBI animals ($p>0.05$ as compared to cohort 1).

Cohort 3. Impact severity was 3.3 ± 0.02 atm. Acute post-TBI mortality was 27% (8/30) ($p>0.05$ as compared with cohorts 1 or 2). The mean post-impact apnea time was 38 ± 3.6 s ($p>0.05$ as compared with cohorts 1 or 2). Post-impact seizure-like behaviors were observed in 30% (9/30) of TBI animals ($p>0.05$ as compared with cohorts 1 or 2).

Blood miR-124-3p levels are increased at 2 d post-TBI

At 2 d post-TBI, blood miR-124-3p levels (cohort 1) in the TBI group were 4.63-fold higher than in the sham-operated experimental controls and 6.92-fold higher than in the 2 months post-TBI group ($p<0.01$, **Fig. 3A**). At 2 months post-TBI, miR-124-3p levels in the TBI group were slightly lower than in sham-operated controls (FC 0.67, $p>0.05$). The ROC analysis indicated that the whole blood miR-124-3p levels (normalized to U6) higher than 0.02 at the 2-d time-point differentiated TBI rats from sham-operated controls with 86% sensitivity and 92% specificity [area under curve (AUC) 0.881, $p<0.01$] **(Fig. 3B)**.

Copy number of plasma miR-124-3p distinguishes TBI rats from controls

As cardiac blood is not a useful route of blood sampling for biomarker studies, we replicated the analysis by assessing plasma sampled from the tail vein in cohort 2. First, to identify the temporal expression pattern of miR-124-3p in plasma, we performed RT-qPCR analysis at baseline, 2 d, 7 d and 3 months post-TBI. The data was normalized to the synthetic spike-in UniSp4. Similar to the U6-normalized whole blood analysis in cohort 1, cohort 2 also revealed an elevation in plasma miR-124-3p levels at 2 d post-TBI. A 1.63-fold increase in plasma miR-124-3p level was observed in the 2 d post-TBI animals in

comparison to sham-operated controls from the same time point ($p<0.05$). In addition, the 2 d post-TBI animals also had elevated plasma miR-124-3p in comparison to their own baseline (FC 2.24, $p<0.01$) or 7 d post-TBI (FC 2.59, $p<0.01$) levels. By 7 d post-TBI, the plasma miR-124-3p level in the injured animals returned to baseline level (7 d post-TBI *vs*. baseline: FC 0.86, $p>0.05$; 3 months post-TBI *vs.* baseline: FC 1.27, $p>0.05$ (**Fig. 3C**).

Next, to perform an absolute quantification of plasma miR-124-3p copy number at 2 d post-TBI, we used ddPCR. The ddPCR analysis in cohort 2 indicated that at 2 d post-TBI, the absolute copy number of plasma miR-124-3p in injured animals was 139% of that in sham-operated controls (44.804 ± 11.66 vs. 32.195 ± 9.95 $p<0.05$; **Fig. 3D**). ROC analysis indicated that a plasma miR-124-3p copy number ≥34/µl (**Fig. 3D**, dashed line) distinguishes injured animals from controls with 89% sensitivity and 67% specificity (AUC 0.815, $p<0.05$; **Fig. 3E**). Moreover, the absolute copy number of miR-124-3p in ddPCR analysis correlated with the UniSp4-normalized RT-qPCR data from the same samples, ($R^2=0.764$, $p<0.01$, **Fig. 3F**). This confirmed that normalizing plasma miR-124-3p RT-qPCR data to the exogenous synthetic spike-in UniSp4 was acceptable, if endogenous normalization controls were not available. Further, both RT-qPCR and ddPCR methodologies reliably detected an increase in the plasma miR-124-3p levels after TBI. Based on these data, plasma RT-qPCR analysis of miR-124-3p levels in cohort 3 was done only at baseline and at 2 d post-TBI.

In cohort 3, hemolysis coefficient of the plasma samples was measured using the ΔC_t (miR-23a - miR-451) method. None of the samples were detected as hemolyzed with this approach, as the hemolysis coefficient was <5 in all samples (**Supplementary tables S1-S3)**.

Pattern of cortical atrophy and extent of perilesional inflammation indicate that lateral FPI causes varied cortical pathologies

MRI analysis of perilesional cortical pathology. Analysis of T2-weighted MRI images was performed from 22 TBI rats (cohort 3) that survived the 2 months post-TBI follow-up. Analysis of cortical lesion in coronal MRI images revealed varying types of cortical pathologies. Some animals showed the presence of a large cortical cavity (**Fig. 4A**) filled with cerebrospinal fluid (**Fig. 4C**), and little or no perilesional T2-enhancement (*i.e.*, edema and inflammatory tissue), while others had a small cortical cavity (**Fig. 4B**) and a wide T2-enhanced perilesional inflammatory rim (**Fig. 4D**). Unfolded maps of two extreme cases are

presented in **Figure 4A-B**. The localization of lesion in the different cytoarchitectonic subfields is described in **Supplementary table S4**.

Nissl staining (**Fig. 4E-F**) revealed differences between the animals in the magnitude of cortical neurodegeneration and distortion in the laminar cytoarchitecture in the region corresponding to the cortical T2-enhancement (**Fig. 4C-D**).

The exact time delay between the TBI impact and the 2 d post-injury plasma sampling was also calculated in this cohort (mean 45±1.4 h, range 43-47 h). There was no correlation between the delay and the miR-124-3p levels (**Fig. 4H**).

Plasma miR-124-3p level at 2 d post-TBI explains the extent of lesion area

The validation cohort (cohort 3) successfully replicated the elevated plasma miR-124-3p level at 2 d post-TBI as compared to controls when the data was normalized to the endogenous control miR-23a. To compare normalized miR-124-3p levels between cohorts 2 and 3 (normalized to exogenous and endogenous controls, respectively), the 2-d miR-124-3p levels were divided by the baseline level of the same animal ($2^{-\Delta Ct\ (2D)}$/ $2^{-\Delta Ct\ (BL)}$). Importantly, elevation in plasma miR-124-3p level at 2 d post-TBI in the validation cohort 3 tolerated the double-normalization approach (FC 1.68, $p<0.05$ as compared to controls, **Fig. 4G**). ROC analysis indicated that the normalized plasma miR-124-3p level of 1.43 distinguished injured animals from controls with 86% sensitivity and 52% specificity (AUC 0.728, $p<0.05$) (**Fig. 4I**).

In cohort 3, we also assessed the effect of different variables, in addition to plasma miR-124-3p on the evolution of cortical pathology. For this, we first calculated a multiple linear regression to explain the chronic lesion area based on plasma miR-124-3p level at 2 d post-TBI, perilesional T2-enhancement, impact pressure, duration of post-injury apnea, animal weight at the time of injury and animal weight at 2 d post-TBI. This six variable model explained the lesion area with R^2 of 0.485, which was not significant owing to the number of independent variables [$F(6, 14) = 2.194$, $p > 0.05$, $R^2 = 0.485$](**Table 1 A,B)**. The level of plasma miR-124-3p at 2 d post-TBI was the only parameter that had a statistically significant linear relation to the lesion area and thus improved the prediction model, $p<0.05$ (**Table 1 C**).

We performed a simple linear regression analysis to provide further insight about the relationship between the plasma miR-124-3p level at 2 d post-TBI and the cortical lesion area at 2 months post-TBI. A linear relationship was observed, indicating that higher the

acute plasma miR-124-3p level, larger the cortical lesion at 2 months post-TBI (R^2=0.327, p<0.01, **Fig. 4J, Table 2 A-C**).

Table 1. Summary of multiple linear regression analysis used to explain chronic lesion area from plasma miR-124-3p at 2 d post-TBI, perilesional T2-enhancement, impact pressure, duration of post-injury apnea, animal weight at the time of injury, and animal weight at 2 d post-TBI.

A

Model Summary

				Change Statistics					
R	R Square	Adjusted R Square	Std. Error of the Estimate	R Square Change	F Change	df1	df2	Sig. F Change	Durbin-Watson
0.696	0.485	0.264	6.970	0.485	2.194	6	14	0.106	2.026

B

ANOVA

Model	Sum of Squares	df	Mean Square	F	Sig.
Regression	639.498	6	106.583	2.194	.106
Residual	680.095	14	48.578		
Total	1319.593	20			

C

Coefficients

	Unstandardized Coefficients		Standardized Coefficients			Collinearity Statistics	
Model	B	Std. Error	Beta	t	Sig.	Tolerance	VIF
(Constant)	-31.746	111.383		-0.285	0.780		
Plasma miR-124-3p at day 2	2.684	1.110	0.496	2.419	**0.030**	0.876	1.142
T2	-0.885	0.556	-0.327	-1.592	0.134	0.873	1.145
Hit pressure	7.077	31.196	0.046	0.227	0.824	0.903	1.108
Apnea	-0.036	0.078	-0.090	-0.454	0.657	0.925	1.081
Weight day 0	0.214	0.205	0.599	1.042	0.315	0.112	8.959
Weight day 2	-0.164	0.207	-0.461	-0.791	0.442	0.108	9.255

Table 2. Summary of simple linear regression analysis used to explain the cortical lesion area at 2 months post-TBI by measuring the plasma miR-124-3p levels at 2 d post-TBI.

A

Model Summary

				Change Statistics					
R	R Square	Adjusted R Square	Std. Error of the Estimate	R Square Change	F Change	df1	df2	Sig. F Change	Durbin-Watson
0.571	0.327	0.291	6.839	0.327	9.215	1	19	0.007	2.354

B

ANOVA

Model	Sum of Squares	df	Mean Square	F	Sig.
Regression	430.980	1	430.980	9.215	0.007
Residual	888.614	19	46.769		
Total	1319.593	20			

C

Coefficients

	Unstandardized Coefficients		Standardized Coefficients			Collinearity Statistics	
Model	B	Std. Error	Beta	t	Sig.	Tolerance	VIF
Lesion area (Constant)	11.008	3.106		3.544	0.002		1.000
Plasma miR-124-3p at day 2	3.093	1.019	0.571	3.036	0.007	1	1.000

Discussion

We tested the hypothesis that the extent of cortical damage after TBI can be explained by circulating brain-enriched miR-124-3p levels. We had two major findings. First, miR-124-3p levels were elevated in both whole cardiac blood and tail vein plasma of rats with TBI, at 2 d post-injury. Second, higher the plasma miR-124-3p level at 2 d post-TBI, greater is the cortical lesion area at 2 months post-TBI.

Lateral FPI induced variable chronic cortical pathology

We present evidence that lateral FPI in adult rats leads to variable progression of the cortical pathologies over the course of 2 months, despite a similar impact type, force, and location. Some rats show massive degeneration of the ipsilateral cortex and mild perilesional T2-enhancement at 2 months post-TBI, suggesting a narrow perilesional inflammatory rim. The rest of the animals exhibited a smaller focal lesion but a wider T2 signal enhancement perilesionally, suggesting long-lasting perilesional inflammation. Development of these pathologies have been consistently observed in our lateral FPI model. We are currently investigating the molecular mechanisms that may explain the variability in the lesion pathology (Ndode-Ekane et al., 2018; Huttunen et al., 2018).

Several previous studies revealed that the development of secondary brain damage after TBI can occur weeks to many months or even years in experimental models and humans (Smith et al., 1997; Johnson et al., 2013; Ramlackhansing et al., 2011). Identification of the course and characteristics of the pathologies in individual subjects after a given impact type has, however remained unexplored, both in animal models and humans with TBI. Based on our data, variability in injury parameters did not explain the variability in the evolution of lesion endophenotype. Interestingly, recent evidence suggests that factors like the stress level of the animal can have a remarkable effect on post-injury outcome (Becker et al., 2015). The contribution of exposomal factors to TBI outcome in individual animals needs to be further explored.

Some studies suggest that the cortical lesion endophenotype can affect the functional outcome in humans. For example, the degree of completeness of glial scarring around cortical iron deposits after a cortical contusion as detected by increased T2 signal in MRI is associated with the development of post-traumatic epilepsy (Messori et al., 2005). Further, the magnitude of blood-brain-barrier damage detected with gadolinium-enhanced MRI rather than cortical lesion size is associated with post-traumatic epilepsy (Tomkins et al., 2008). Identification of prognostic biomarkers that would associate with the evolution of the

tissue pathology would not only help to stratify patient populations with the greatest need for treatment, but also facilitate the selection of treatment targets.

Circulating miR-124-3p is a prognostic biomarker for the evolution of the cortical pathology

Human studies aimed at identifying miRNAs as predictive and/or prognostic biomarkers for disease mechanisms often implement a multi-cohort study design (Takahashi et al., 2015; Pedroza-Torres et al., 2016, Devaux et al., 2016). A discovery cohort is used to identify miRNAs altered in a particular pathological condition. A validation cohort is then used to replicate the data and confirm the biomarker value of the selected candidates (Takahashi et al., 2015; Pedroza-Torres et al., 2016, Devaux et al., 2016).

Consistent with human biomarker discovery studies, we performed a multi-cohort analysis to validate miR-124-3p as a biomarker for TBI and progression of the cortical pathology. First, we demonstrated elevated miR-124-3p levels in whole blood and plasma at 2 d post-TBI in two animal cohorts. We then validated the findings by demonstrating increased plasma miR-124-3p levels at 2 d post-TBI in an independent validation cohort. Importantly, the results were comparable in cardiac whole blood and tail vein plasma. We also showed in the validation cohort that higher plasma miR-124-3p levels at 2 d post-TBI explained the development of a larger chronic cortical lesion area at 2 months post-TBI. In addition to the magnitude of cortical tissue loss, another characteristic of the cortical lesion is the presence of perilesional T2 signal enhancement, indicating tissue edema and inflammation (Van Putten et al., 2005; Wang et al., 2017). Our data indicate that the chronically developed lesion area exhibits a linear relationship with the acute circulating plasma miR-124-3p level, but not with the T2-enhancement. In addition, none of the other parameters measured in this study, such as the impact pressure, duration of post-injury apnea, weight at the time of injury, or weight at 2 d post-TBI could explain the chronic lesion area development.

miR-124-3p is a brain-enriched miRNA (Mishima et al., 2007; Lagos-Quintana et al., 2002) expressed primarily in neurons (Smirnova et al., 2005). As TBI causes disruption of brain tissue and leakage from the blood-brain barrier, as well as increased permeability of the blood-brain barrier (Başkaya et al., 1997; Li et al., 2016), we propose that increased plasma miR-124-3p levels at 2 d TBI indicate massive ongoing neurodegeneration. We consider that elevated plasma miR-124-3p levels at 2 d post-TBI could be used as a

prognostic biomarker for the evolution of large cortical lesion, and consequently, applied for stratification of animals for neuroprotective treatment trials.

However, it should be noted that increased post-injury plasma miR-124 levels as a biomarker for neurodegeneration is not TBI-specific. In stroke models, acute elevation in circulating miR-124 levels has often been observed, for instance, at 6-48 h post-stroke (Laterza et al., 2009; Weng et al., 2011; Leung et al., 2014; Rainer et al., 2016). Furthermore, Leung et al. (Leung et al., 2014) showed that miR-124 can be used as biomarker to differentiate hemorrhagic and ischemic stroke patients at 6 h post-stroke. In addition, serum exosomal miR-124 levels can be used as a biomarker for acute ischemic stroke, with the miR-124 levels positively correlating with infarct volume (Ji et al., 2016). A recent study from CSF analysis of patients with acute ischemic stroke has revealed elevated miR-124-3p particularly in patients with infarct size > 2 cm^3 (Sørensen et al., 2017).

Thus, our findings indicate that the expression pattern of circulating miR-124-3p in response to brain injury is similar in TBI and stroke, with higher circulating miR-124-3p levels associating with greater perilesional tissue damage.

Methodological considerations

The mortality rate in our study involving three separate study cohorts ranged from 0-27%. Based on our previous experience, we expected a 20-30% mortality at the impact atm levels used (about 3.2 atm). However, the acute TBI-induced mortality (death in <72 hr) in the whole group of 57 injured rats included in the present study was only 16% (9/57). In particular, the 1st two cohorts with low number of injured animals (17 and 10, respectively) had low mortality rates (6% and 0%, respectively). In other multi-cohort studies performed in our laboratory, involving >100 rats per study (about 15-20 rats per cohort), we have also observed a cohort-dependent variability in mortality, even though the injuries were performed by the same very experienced technician (Nissinen et al., 2017 : 323 TBI animals, 13 cohorts, total mortality 20%, inter-cohort variability in mortality 7-42%; Mitchell et al., 2008: 214 TBI animals, 8 cohorts, total mortality 15%, inter-cohort variability in mortality 0-30%). Most importantly, the mortality in our 3rd cohort that was used for validation of plasma miR-124-3p data from cohorts 1 and 2, and for the identification of the cortical pathologies was as expected (27%). This data strengthens the reproducibility of our observations, as miR-124-3p at acute post-TBI phase were elevated independent of the cohort-specific differences in mortality.

The anesthesia cocktail used in our cohorts 2 and 3 for plasma sampling also slightly differed from the cohort 1, since chloral hydrate was omitted based on the license instructions. However, all three cohorts demonstrated the miR-124-3p peak in circulation at 2 d post-TBI, indicating that the miRNA tolerates experimental variability, and the acute elevation of the miRNA level in plasma is not influenced by the anesthesia composition.

Synthetic miRNAs added to *ex vivo* plasma become rapidly degraded by endogenous RNases, whereas endogenous circulating miRNAs, such as plasma miR-124-3p sustain temperature-related changes and long-term storage at room temperature, (Chen et al., 2008; Vickers et al., 2011). This raises a question, how brain-derived miR-124-3p can still be detected in the circulation at 2 d post-TBI? The prevailing hypothesis is that the circulating miRNAs are protected by their encapsulation into extracellular vesicles or by binding to proteins (Mitchell et al., 2008) or high-density lipoprotein particles (Lunavat et al., 2015). This is supported by studies in humans showing that miR-124-3p is found in plasma exosomes (Huang et al., 2013); although there is evidence that in rats circulating miR-124 is bound to proteins rather than extracellular vesicles (Karttunen et al., 2019).

The identification of reliable circulating miRNA biomarkers is also susceptible to methodologic artifacts involved during serum/plasma sampling. For example, the release of miRNAs from blood cells during serum/plasma isolation can affect quantitative analysis. Previously, Shah et al. (Shah et al., 2016) compared several methods for detecting hemolysis in human serum samples, including visual inspection, measurement of hemoglobin absorbance by spectrophotometry at 414 nm, measurement of hemoglobin using a Coulter®AcT diff™Analyzer, and the ratio of red blood cell-enriched miR-451 to a reference miRNA, miR-23a. They found that the miR-451/miR-23a ratio was the most sensitive indicator of hemolysis. Blondal et al. (2013) found that a ΔC_t value ≥ 5 for miR-451/miR-23a ratio indicates possible erythrocyte miRNA contamination, and a ΔC_t of ≥7 indicates a high risk of hemolysis. Based on analysis of the miR-451/miR-23a ratio and ΔC_t (miR-23a - miR-451), none of our cohort 3 samples were hemolysed, excluding its contribution to the measured plasma miR-124-3p levels.

Identification of reliable circulating miRNA biomarkers is complicated due to the lack of suitable endogenous controls. In our study, absolute copy numbers of plasma miR-124-3p as well as exogenous, endogenous and baseline normalization methods consistently revealed elevation in post-TBI miR-124-3p levels in the whole blood and plasma samples, indicating no implicit bias due to the different normalization strategies.

Thus, the most important finding from our study was that miR-124-3p levels increased in all three independent animal cohorts after TBI, regardless of: (i) whether we analyzed cardiac whole blood or tail vein plasma, and (ii) the experimental variabilities involved. Moreover, the miRNA level was particularly higher in the animals with large lesion area at 2 d post-TBI in comparison to the animals with small lesion area.

Our findings indicate that lateral FPI leads to the development of cortical pathologies that differ in the chronic lesion area. Further, plasma level of the brain enriched miR-124-3p is elevated at 2 d post-TBI, and this acute elevation associates linearly with the extent of the chronic loss of cortical tissue. We propose that analysis of plasma miR-124-3p levels provides a non-invasive prognostic biomarker for the evolution of the cortical pathology.

Conflict of interest

The authors declare no conflict of interest.

Author contribution

N.V.,S.D.G., N.P., and A.P. Designed the research.

N.P., N.V.,S.D.G. Performed research.

N.V.,S.D.G., R.H., J.T. and N.P. Analyzed data.

N.V.,S.D.G., and A.P. Wrote the paper with input from all authors.

Acknowledgement

We thank Mr. Jarmo Hartikainen and Mrs. Merja Lukkari for their excellent technical assistance. This study was supported by the Medical Research Council of the Academy of Finland (Grants 272249, 273909 and 317203) and by the European Union's Seventh Framework Programme (FP7/2007-2013) under grant agreement n°602102 (EPITARGET).

References

Åkerblom, Malin, et al. "MicroRNA-124 is a subventricular zone neuronal fate determinant." The Journal of Neuroscience 32.26 (2012): 8879-8889.

Andrade P, Ciszek R, Pitkänen A, Ndode-Ekane XE. A web-based application for generating 2D-unfolded cortical maps to analyze the location and extent of cortical lesions following traumatic brain injury in adult rats. J Neurosci Methods 2018;308:330-336.

Bartel DP. MicroRNAs: genomics, biogenesis, mechanism, and function. Cell. 2004; 116(2):281-97.

Başkaya MK, Muralikrishna Rao A, Doğan A, Donaldson D, Dempsey RJ. The biphasic opening of the blood–brain barrier in the cortex and hippocampus after traumatic brain injury in rats. Neuroscience Letters. 1997 Apr 18;226(1):33–6.

Bayr H, Clark RS, Kochanek PM. Promising strategies to minimize secondary brain injury after head trauma. Critical care medicine. 2003 Jan 1;31(1):S112-7.

Becker C, Bouvier E, Ghestem A, Siyoucef S, Claverie D, Camus F, et al. Predicting and treating stress-Induced vulnerability to epilepsy and depression. Ann Neurol 2015;78(1):128-136.

Bigler ED (2001) The lesion(s) in traumatic brain injury: implications for clinical neuropsychology. Arch Clin Neuropsychol. 16(2):95-131.

Blondal T, Jensby N, Baker A, Andreasen D, Mouritzen P, Wrang T, et al. Assessing sample and miRNA profile quality in serum and plasma or other biofluids. Methods. 2013;59(1):164–9.

Bot, Anna Maria, Konrad Józef Dębski, and Katarzyna Lukasiuk. "Alterations in miRNA levels in the dentate gyrus in epileptic rats." PLoS One 8.10 (2013): e76051.

Bramlett HM, Dietrich WD. Long-term consequences of traumatic brain injury: current status of potential mechanisms of injury and neurological outcomes. Journal of neurotrauma. 2015 Dec 1;32(23):1834-48.

Carvalho-Gaspar, Manuela, et al. "Chemokine gene expression during allograft rejection: comparison of two quantitative PCR techniques." Journal of immunological methods 301.1 (2005): 41-52.

Chen X, Ba Y, Ma L, Cai X, Yin Y, Wang K, Guo J, Zhang Y, Chen J, Guo X, Li Q, Li X, Wang W, Zhang Y, Wang J, Jiang X, Xiang Y, Xu C, Zheng P, Zhang J, Li R, Zhang H, Shang X, Gong T, Ning G, Wang J, Zen K, Zhang J, Zhang CY (2008) Characterization of microRNAs in serum: a novel class of biomarkers for diagnosis of cancer and other diseases. Cell Res. 2008 Oct;18(10):997–1006.

Chen, Teng, et al. "Downregulation of microRNA-124 predicts poor prognosis in glioma patients." Neurological Sciences 36.1 (2015): 131-135.

Cheng, Li-Chun, et al. "miR-124 regulates adult neurogenesis in the subventricular zone stem cell niche." Nature neuroscience 12.4 (2009): 399-408.

Devaux, Yvan, et al. "Association of circulating MicroRNA-124-3p levels with outcomes after out-of-hospital cardiac arrest: a substudy of a randomized clinical trial." Jama cardiology 1.3 (2016): 305-313.

Ekolle Ndode-Ekane X, Kharatishvili I, Pitkänen A. Unfolded Maps for Quantitative Analysis of Cortical Lesion Location and Extent after Traumatic Brain Injury. J Neurotrauma 2017;34(2):459-474.

Gundersen HJG, Bagger P, Bendtsen TF, Evans SM, Korbo L, Marcussen N, et al. The new stereological tools: Disector, fractionator, mucleator and point sampled intercepts and their use in pathological research and diagnosis. APMIS. 1988;96(10):857–81.

Gundersen HJG, Bendtsen TF, Korbo L, Marcussen N, Moller A, Nielsen K, et al. Some new, simple and efficient stereological methods and their use in pathological research and diagnosis. APMIS. 1988;96(5):379–94.

Hata, Tissa R., et al. "Administration of oral vitamin D induces cathelicidin production in atopic individuals." The Journal of allergy and clinical immunology 122.4 (2008): 829.

Huang X, Yuan T, Tschannen M, Sun Z, Jacob H, Du M, et al. Characterization of human plasma-derived exosomal RNAs by deep sequencing. BMC Genomics. 2013 May 10;14:319.

Huttunen JK, Airaksinen AM, Barba C, Colicchio G, Niskanen JP, Shatillo A, Sierra Lopez A, Ndode-Ekane XE, Pitkanen A, Gröhn O (2018) Detection of Hyperexcitability by fMRI After Experimental Traumatic Brain Injury. J Neurotrauma. 2018 Jul 18. doi: 10.1089/neu.2017.5308. [Epub ahead of print]

Huusko N, Römer C, Ndode-Ekane XE, Lukasiuk K, Pitkänen A (2013) Loss of hippocampal interneurons and epileptogenesis: a comparison of two animal models of acquired epilepsy. Brain Struct Funct. 2015 Jan;220(1):153-91. doi: 10.1007/s00429-013-0644-1. Epub 2013 Oct 6.

Ji Q, Ji Y, Peng J, Zhou X, Chen X, Zhao H, et al. Increased brain-specific MiR-9 and MiR-124 in the serum exosomes of acute ischemic stroke patients. PLoS ONE. 2016;11(9).

Johnson VE, Stewart JE, Begbie FD, Trojanowski JQ, Smith DH, Stewart W (2013) Inflammation and white matter degeneration persist for years after a single traumatic brain injury. Brain. 2013 Jan;136(Pt 1):28-42. doi: 10.1093/brain/aws322.

Karttunen J, Heiskanen M, Navarro-Ferrandis V, Das Gupta S, Lipponen A, Puhakka N, et al. Precipitation-based extracellular vesicle isolation from rat plasma co-precipitate vesicle-free microRNAs. J Extracell Vesicles 2019;8(1).

Kersel DA, Marsh NV, Havill JH, Sleigh JW. Neuropsychological functioning during the year following severe traumatic brain injury. Brain injury. 2001 Jan 1;15(4):283-96.

Kharatishvili I, Nissinen JP, McIntosh TK, Pitkänen A (2006) A model of posttraumatic epilepsy induced by lateral fluid-percussion brain injury in rats. Neuroscience. 140:685–97.

Lagos-Quintana M, Rauhut R, Yalcin A, Meyer J, Lendeckel W, Tuschl T. Identification of Tissue-Specific MicroRNAs from Mouse. Current Biology. 2002 Apr 30;12(9):735–9.

Laterza OF, Lim L, Garrett-Engele PW, Vlasakova K, Muniappa N, Tanaka WK, et al. Plasma MicroRNAs as Sensitive and Specific Biomarkers of Tissue Injury. Clinical Chemistry. 2009 Nov 1;55(11):1977–83.

Leung LY, Chan CPY, Leung YK, Jiang HL, Abrigo JM, Wang DF, et al. Comparison of miR-124-3p and miR-16 for early diagnosis of hemorrhagic and ischemic stroke. Clinica Chimica Acta. 2014 Jun 10;433:139–44.

Li W, Watts L, Long J, Zhou W, Shen Q, Jiang Z, et al. Spatiotemporal changes in blood-brain barrier permeability, cerebral blood flow, T2 and diffusion following mild traumatic brain injury. Brain Research. 2016 Sep 1;1646:53–61.

Lunavat TR, Cheng L, Kim D-K, Bhadury J, Jang SC, Lässer C, et al. Small RNA deep sequencing discriminates subsets of extracellular vesicles released by melanoma cells--Evidence of unique microRNA cargos. RNA Biol. 2015;12(8):810–23.

Maru, Dipen M., et al. "MicroRNA-196a is a potential marker of progression during Barrett's metaplasia-dysplasia-invasive adenocarcinoma sequence in esophagus." The American journal of pathology 174.5 (2009): 1940-1948.

McAllister (2011) Neurobiological consequences of traumatic brain injury. Dialogues Clin Neurosci. 13(3): 287–300.

McIntosh TK, Vink R, Noble L, Yamakami I, Fernyak S, Soares H, Faden AL (1989) Traumatic brain injury in the rat: Characterization of a lateral fluid-percussion model. Neuroscience. 28:233–44.

Messori, A, Polonara, G, Carle, F, Gesuita, R, Salvolini, U (2005) Predicting posttraumatic epilepsy with MRI: Prospective longitudinal morphologic study in adults. Epilepsia. 2005 Sep;46(9):1472-81

Mishima T, Mizuguchi Y, Kawahigashi Y, Takizawa T, Takizawa T. RT-PCR-based analysis of microRNA (miR-1 and -124) expression in mouse CNS. Brain Research. 2007 Feb 2;1131:37–43.

Mitchell PS, Parkin RK, Kroh EM, Fritz BR, Wyman SK, Pogosova-Agadjanyan EL, et al. Circulating microRNAs as stable blood-based markers for cancer detection. PNAS. 2008 Jul 29;105(30):10513–8.

Ndode-Ekane XE, Matthiesen L, Bañuelos-Cabrera I, Palminha CAP, Pitkänen A (2018) T-cell infiltration into the perilesional cortex is long-lasting and associates with poor somatomotor recovery after experimental traumatic brain injury. Restor Neurol Neurosci. 2018;36(4):485-501. doi: 10.3233/RNN-170811.

Nissinen J, Andrade P, Natunen T, Hiltunen M, Malm T, Kanninen K, Soares JI, Shatillo O, Sallinen J, Ndode-Ekane XE, Pitkänen A (2017) Disease-modifying effect of atipamezole in a model of post-traumatic epilepsy. Epilepsy Res. 2017 Oct;136:18-34. doi: 10.1016/j.eplepsyres.2017.07.005. Epub 2017 Jul 12.

Paxinos G & Watson C (2007) The Rat Brain in Stereotactic Coordinates, Sixth Edition. Academic Press, INC., San Diego, California.

Pedroza-Torres, Abraham, et al. "A microRNA expression signature for clinical response in locally advanced cervical cancer." Gynecologic Oncology 142.3 (2016): 557-565.

Peng, Jing, et al. "Expression patterns of miR-124, miR-134, miR-132, and miR-21 in an immature rat model and children with mesial temporal lobe epilepsy." Journal of Molecular Neuroscience 50.2 (2013): 291-297.

Rainer TH, Leung LY, Chan CPY, Leung YK, Abrigo JM, Wang D, et al. Plasma miR-124-3p and miR-16 concentrations as prognostic markers in acute stroke. Clinical Biochemistry. 2016 Jun;49(9):663–8.

Ramlackhansingh AF, Brooks DJ, Greenwood RJ, Bose SK, Turkheimer FE, Kinnunen KM, Gentleman S, Heckemann RA, Gunanayagam K, Gelosa G, Sharp DJ (2011) Inflammation after trauma: microglial activation and traumatic brain injury. Ann Neurol. 2011 Sep;70(3):374-83. doi: 10.1002/ana.22455. Epub 2011 Jun 27

Savelyeva AV, Kuligina EV, Bariakin DN, Kozlov VV, Ryabchikova EI, Richter VA, et al. Variety of RNAs in Peripheral Blood Cells, Plasma, and Plasma Fractions. BioMed Research International. 2017;2017.

Schmitz C, Hof PR. Design-based stereology in neuroscience. Neuroscience. 2005;130(4):813–31.

Sempere LF, Freemantle S, Pitha-Rowe I, Moss E, Dmitrovsky E et al. (2004) Expression profiling of mammalian microRNAs uncovers a subset of brain-expressed microRNAs with possible roles in murine and human neuronal differentiation. Genome Biol 5: R13. doi:10.1186/gb-2004-5-3-r13. PubMed: 15003116.

Shah JS, Soon PS, Marsh DJ. Comparison of Methodologies to Detect Low Levels of Hemolysis in Serum for Accurate Assessment of Serum microRNAs. PLOS ONE. 2016 Apr 7;11(4):e0153200.

Smirnova L, Gräfe A, Seiler A, Schumacher S, Nitsch R, Wulczyn FG. Regulation of miRNA expression during neural cell specification. Eur J Neurosci. 2005 Mar;21(6):1469–77.

Smith DH, Chen X-H, Pierce JES, Wolf JA, Trojanowski JQ, Graham DI, et al. Progressive atrophy and neuron death for one year following brain trauma in the rat. Journal of Neurotrauma. 1997;14(10):715–27.

Sofie Sølvsten Sørensen, Ann-Britt Nygaard, Anting Liu Carlsen, Niels H. H. Heegaard, Mads Bak, and Thomas Christensen (2017) Elevation of brain-enriched miRNAs in cerebrospinal fluid of patients with acute ischemic stroke. Biomark Res. 2017; 5: 24. doi: 10.1186/s40364-017-0104-9

Song, Jianning, et al. "Identification of suitable reference genes for qPCR analysis of serum microRNA in gastric cancer patients." Digestive diseases and sciences 57.4 (2012): 897-904.

Synnot A, Gruen RL, Menon D, Steyerberg EW, Buki A, Peul WC, Elliott JH, Maas A. A new approach to evidence synthesis in traumatic brain injury: A living systematic review. Journal of neurotrauma. 2015 Sep 28.

Takahashi, Ikuko, et al. "Identification of plasma microRNAs as a biomarker of sporadic Amyotrophic Lateral Sclerosis." Molecular brain 8.1 (2015): 67.

Tang G, Shen X, Lv K, Wu Y, Bi J, Shen Q. Different Normalization Strategies Might Cause Inconsistent Variation in Circulating microRNAs in Patients with Hepatocellular Carcinoma. Med Sci Monit. 2015 Feb 26;21:617–24.

Taylor CA, Bell JM, Breiding MJ, Xu L. (2017) Traumatic brain injury–related emergency department visits, hospitalizations, and deaths—United States, 2007 and 2013. MMWR. Surveillance Summaries. 2017;66 (9):1-16. doi: 10.15585/mmwr.ss6609a1.

Tian, Yao, et al. "Interaction of serum microRNAs and serum folate with the susceptibility to pancreatic cancer." Pancreas 44.1 (2015): 23-30.

Tomkins O, Shelef I, Kaizerman I, Eliushin A, Afawi Z, Misk A, Gidon M, Cohen A, Zumsteg D, Friedman A (2008) Blood-brain barrier disruption in post-traumatic epilepsy. J Neurol Neurosurg Psychiatry. 2008 Jul;79(7):774-7. Epub 2007 Nov 8.

Van Putten HP, Bouwhuis MG, Muizelaar JP, Lyeth BG, Berman RF (2005) Diffusion-weighted imaging of edema following traumatic brain injury in rats: effects of secondary hypoxia. J Neurotrauma. 22(8):857-72.

Vickers KC, Palmisano BT, Shoucri BM, Shamburek RD, Remaley AT. MicroRNAs are transported in plasma and delivered to recipient cells by high-density lipoproteins. Nat Cell Biol. 2011 Apr;13(4):423–33.

Visvanathan, Jaya, et al. "The microRNA miR-124 antagonizes the anti-neural REST/SCP1 pathway during embryonic CNS development." Genes & development 21.7 (2007): 744-749.

Wang W, Zhang H, Lee DH, Yu J, Cheng T, Hong M, Jiang S, Fan H, Huang X, Zhou J, Wang J (2017) Using functional and molecular MRI techniques to detect neuroinflammation and neuroprotection after traumatic brain injury. Brain Behav Immun. 64:344-353. doi: 10.1016/j.bbi.2017.04.019.

Wang, Jin, Jinyun Chen, and Subrata Sen. "MicroRNA as biomarkers and diagnostics." Journal of cellular physiology 231.1 (2016): 25-30.

Weber JA, Baxter DH, Zhang S, Huang DY, Huang KH, Lee MJ, et al. The microRNA spectrum in 12 body fluids. Clinical chemistry. 2010; 56(11):1733±41. doi: 10.1373/clinchem.2010.147405 PMID: 20847327

Weng H, Shen C, Hirokawa G, Ji X, Takahashi R, Shimada K, et al. Plasma miR-124 as a biomarker for cerebral infarction. Biomedical Research. 2011;32(2):135–41.

Xiang M, Zeng Y, Yang R, Xu H, Chen Z, Zhong J, et al. U6 is not a suitable endogenous control for the quantification of circulating microRNAs. Biochem Biophys Res Commun. 2014 Nov 7;454(1):210–4.

Yan Y, Wang C, Zhou W, Shi Y, Guo P, Liu Y, et al. Elevation of Circulating miR-210-3p in High-Altitude Hypoxic Environment. Front Physiol [Internet]. 2016 [cited 2017 Mar 14];7. Available from: http://journal.frontiersin.org/article/10.3389/fphys.2016.00084/abstract

Figure Legends

Fig. 1. Flow-chart of the study. (A) A flow chart showing the number of animals and acute (<72 h) mortality in the three cohorts of rats with sham-operation or lateral fluid-percussion (FPI) induced traumatic brain injury (TBI). Cohort 1: a discovery cohort to assess miR-124-3p in whole blood. Cohort 2: a discovery cohort used to assess miR-124-3p in plasma at different post-TBI time points. Cohort 3: a validation cohort to confirm the elevation in plasma miR-124-3p and assess its association with chronic development of cortical lesion. **(B)** Study design showing the timing of blood sampling and duration of follow-up. *Abbreviations: d, days; ddPCR, droplet digital PCR; FPI, fluid percussion injury; MRI, magnetic resonance imaging; NISSL, Nissl staining; RT-qPCR, reverse transcriptase quantitative polymerase chain reaction; sham, sham-operated control rat.*

Fig. 2. Regions of interest used to calculate cortical volumes. (**A**) Vertical lines placed on the sagittal Nissl-stained section show the rostrocaudal extent of the brain; 1-mm coronal MRI slices were used to measure the volume of the remaining cortex and perilesional inflammatory rim. (**B**) A coronal T2-weighted MRI slice showing the outlines of the regions of interests. Abbreviations: A_{infl}, area of T2 enhancement, suggesting edema and ongoing inflammatory response; CX_{contra}, volume of contralateral cortex; CX_{ipsi}, volume of ipsilateral cortex; Hc, hippocampus; rf, rhinal fissure; Tha, thalamus; TBI, traumatic brain injury; V, lateral ventricle. Scale bar, 2 mm.

Fig. 3. Increased circulating miR-124-3p levels at 2 d post-injury differentiate TBI rats from controls. (A) At 2 d post-TBI, RT-qPCR analysis indicated an increase in cardiac blood miR-124-3p levels (cohort 1) as compared to that in controls (FC 4.63, $p<0.01$) or TBI animals at 2 months post-injury (FC 6.92, $p<0.01$). At 2 months post-TBI, injured animals did not differ from controls (FC 0.67, $p>0.05$). **(B)** ROC analysis indicated that at 2 d post-TBI, cardiac whole blood miR-124-3p is a sensitive and specific diagnostic biomarker for TBI (AUC 0.881, $p<0.01$). **(C)** RT-qPCR analysis from tail vein plasma (cohort 2) revealed a similar peak in miR-124-3p levels at 2 d post-TBI in comparison to sham-operated controls, normalizing to baseline by 7 d post-TBI (2 d TBI vs. sham: FC 1.63, $p<0.05$; 2 d TBI vs. baseline TBI: FC 2.24, $p<0.01$; 2 d TBI vs. 7 d TBI: FC 2.59, $p<0.01$). **(D)** DdPCR analysis at 2 d post-TBI (cohort 2) conformed with the RT-qPCR finding, indicating a 1.39-fold increase in tail vein plasma miR-124-3p level in the TBI rats in comparison to sham-operated controls ($p<0.05$). The dashed line indicates the threshold plasma miR-124-3p concentration

(34 miR-124-3p copies/µl plasma) required to distinguish TBI animals from controls with 89% sensitivity and 67% specificity. **(E)** ROC analysis from plasma ddPCR indicated that at 2 d post-TBI, tail vein plasma miR-124-3p is also a sensitive and specific diagnostic biomarker for TBI (AUC 0.815, $p<0.05$). **(F)** Linear regression analysis for tail vein plasma miR-124-3p copy number measured in cohort 2 with ddPCR with the corresponding RT-qPCR measurements from the same samples indicated that both RT-qPCR and ddPCR can be reliably used to quantify its plasma levels ($R^2=0.764$, $p<0.01$). *Abbreviations: AUC, area under curve; BL, baseline; Ct, cycle threshold, d, days; ddPCR, droplet digital polymerase chain reaction; mo, months; RT-qPCR, reverse transcriptase quantitative polymerase chain reaction; S, sham-operated control; T, TBI-induced animal. One TBI animal was excluded from cohort 2 due to a high standard deviation between technical replicates in ddPCR analysis).*

Fig. 4. Representative examples of lesion extent and perilesional inflammation at two months after lateral fluid-percussion injury. Unfolded cortical maps and coronal T2-weighted magnetic resonance images (MRI) from representative rats with a large cortical cavity **(A, C)** or a small focal cortical lesion **(B, D)**. Blue shading indicates the cortical lesion. **(E-F)** Nissl stained sections showing cytoarchitectonics of the cortical areas of perilesional T2-enhancement in cases shown in panels C-D. **(G)** Similar to cohort 2, tail vein plasma miR-124-3p was upregulated (FC 1.68, $p<0.05$) at 2 d post-TBI in MRI cohort (cohort 3), **(H)** A 43-47 hour variability in sampling time did not affect the miR-124-3p levels. **(I)** The ROC analysis indicated that at 2 d post-TBI, plasma miR-124-3p is a sensitive and specific diagnostic biomarker for TBI (AUC 0.728, $p<0.05$). A simple linear regression was calculated to explain lesion area based on tail vein plasma miR-124. **(J)** A significant regression was found with R^2 of 0.327 ($p<0.01$). *Abbreviations: AUC, area under curve; BL, baseline; Ct, cycle threshold, D, days; nissl, Nissl staining; TBI, traumatic brain injury. Scale bar in panel E equals 200 µm. One TBI animal was excluded from cohort 3 due to a high standard deviation between technical replicates in RT-qPCR analysis.*

Highlights

- Evolution of cortical pathology after lateral fluid-percussion injury is variable
- Characteristics of primary impact do not explain variability in the evolution of cortical pathology
- Plasma miR-124-3p level presents a prognostic biomarker for the evolution of cortical pathology

A

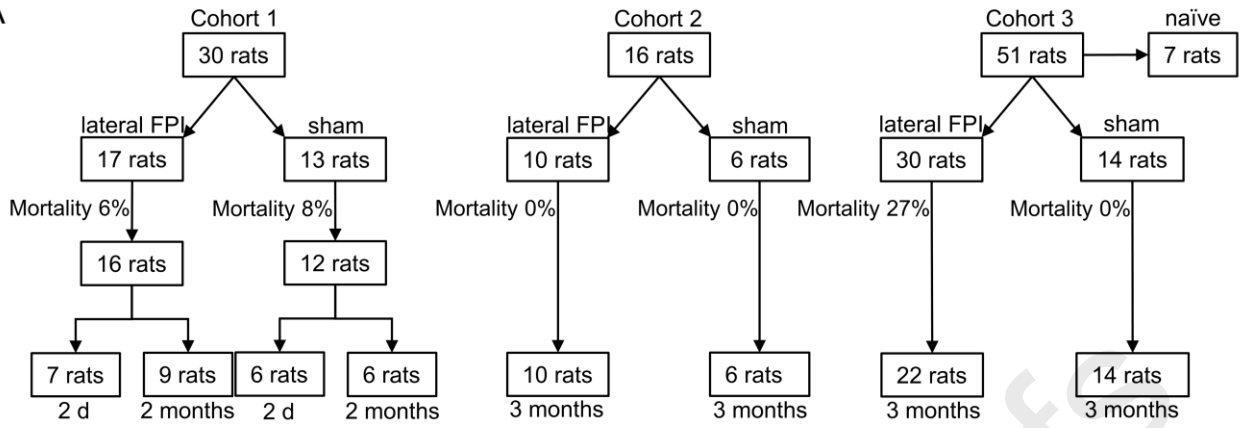

B